ELSEVIER

Journal of Fluids and Structures 20 (2005) 1007–1023

JOURNAL OF FLUIDS AND STRUCTURES

www.elsevier.com/locate/jfs

Numerical flow models to simulate tuned liquid dampers (TLD) with slat screens

M.J. Tait[a], A.A. El Damatty[b,*], N. Isyumov[b], M.R. Siddique[b]

[a]*Department of Civil Engineering, McMaster University, Hamilton, Ont., Canada L8S 4L7*
[b]*Department of Civil and Environmental Engineering, University of Western Ontario, London, Ont., Canada N6A 5B9*

Received 11 August 2004; accepted 6 April 2005
Available online 11 July 2005

Abstract

The tuned liquid damper (TLD) is increasingly being used as an economical and effective dynamic vibration absorber to mitigate the dynamic response of structures. In this paper the results of two numerical flow models of TLD behaviour are compared with experimental data. These include the free surface motion, the resulting base shear forces, and the energy dissipated by a TLD with slat screens. The importance of this experimental study is that it examines TLD behaviour over a large range of normalized excitation amplitude values, covering the practical range of serviceability accelerations for buildings subjected to wind loads and larger excitation amplitudes more representative of earthquake motion. In addition, the experimental results are used to assess the models for larger fluid depth to tank length values, and for the use of modelling TLDs equipped with multiple screens. For screens consisting of a number of thin plate slats, a method for determining the loss coefficient is presented, which is a required parameter for the models used in this paper. Findings indicate that the linear model is capable of providing an initial estimate of the energy dissipating characteristics of a TLD. The nonlinear model can accurately describe the response characteristics within the range of excitation amplitudes experimentally tested.

Keywords: Tuned liquid damper; Damping; Screens; Vibration; Absorber; Dynamic

1. Introduction

A properly designed partially filled water tank can be utilized as a vibration absorber to reduce the dynamic motion of a structure and is referred to as a tuned liquid damper (TLD). The design parameters of a TLD-structure system are: (a) the mass ratio, μ, defined as the ratio of the effective mass of the fluid to the generalized mass of the structure corresponding to the mode to be suppressed, (b) the natural frequency of the liquid sloshing motion, f_w, and (c) the inherent damping of the TLD, ζ_{TLD}. Typically, values of μ for tall structures range between approximately 1% and 5%. Using linear wave theory, the natural frequency of the sloshing motion can be evaluated as a function of the tank length and the fluid depth. The TLD is tuned such that its fundamental sloshing frequency nearly matches the natural frequency of the structure's vibration mode of interest.

*Corresponding author. Tel.: +1 519 661 2139; fax: +1 519 661 3779.
E-mail address: damatty@uwo.ca (A.A. El Damatty).

0889-9746/$ - see front matter © 2005 Published by Elsevier Ltd.
doi:10.1016/j.jfluidstructs.2005.04.004

The optimum inherent damping value depends on the value of μ. Expressions to determine the optimum damping of a linear tuned mass damper (TMD) as a function of μ have been derived by Warburton (1982). Due to the analogy between TLD and TMD, such an expression can be adopted for TLDs by replacing the solid mass of the TMD with the effective mass of the fluid. The optimum inherent damping values, corresponding to typical mass ratio values, range between approximately 5% and 15%. The main source of damping for a TLD without additional damping devices arises from viscous dissipation in the boundary layers at the walls and bottom of the tank and from free surface contamination (Miles, 1967). The inherent damping, ζ_{TLD}, for a TLD without additional energy dissipating devices is usually significantly less than optimal, resulting in a less effective vibration absorber. Additionally, the response of an underdamped TLD is more nonlinear and less controllable, reducing its reliability. Often the TLD is used as a water storage tank preventing the use of a higher-viscosity liquid. Several approaches have been implemented to increase the energy dissipated by the sloshing fluid, including roughness elements (Fujino et al., 1988), surface contaminants (Tamura et al., 1995), wave breaking in shallow water TLDs (Sun et al., 1992), and nets or screens (Welt, 1983; Noji et al., 1988; Warnitchai and Pinkaew, 1998; Kaneko and Ishikawa, 1999). The damping devices selected for this study to increase ζ_{TLD} consist of horizontal slats uniformly spaced apart in order to form screens. The use of this particular screen arrangement allows the space between the slats to be varied until the targeted amount of damping is achieved.

Simulation of the response behaviour of a TLD equipped with slat screens can be carried out using either linear or nonlinear numerical flow models that are available in the literature. An experimental program is conducted and the results are used to assess the ability of both a linear and a nonlinear model to simulate the free surface motion, the resulting base shear force and the energy dissipated by a TLD equipped with slat screens. The new contribution of this experimental study is that it validates the above numerical models under larger excitation amplitudes, A, larger fluid depth, h, to tank length, L, ratio values, and for the use of multiple screens in the nonlinear model. Specifically, the experimental results are used to assess the adequacy of the model(s) in predicting the sloshing behaviour for the following cases.

(i) Tanks subjected to both small and large excitation amplitudes that correspond to small motions associated with wind loads and large motions more representative of earthquake excitation. Kaneko and Ishikawa (1999) have validated the nonlinear model for an A/L of 0.0025, whereas in this study the TLD is tested over $0.0026 < A/L < 0.0414$. The upper bound of excitation amplitude ratio applied in this study exceeds the maximum amplitude ratio tested by Kaneko and Ishikawa (1999) by more than an order of magnitude.
(ii) Tanks with the ratio of water depth, h, to tank length, L, values that cover a range of practical h/L values. The use of higher h/L values has the advantage of reducing the space requirements. In this study the nonlinear model is validated for an h/L value approximately 1.5 times larger than previously considered.
(iii) Tanks fitted with multiple damping slat screens. The purpose is to assess if the nonlinear model can adequately simulate the response of a TLD equipped with multiple slat screens.

In both numerical models, the effect of the screens is simulated through a loss coefficient. An experimental program is conducted to determine the loss coefficient of slat screens. An approach for predicting this coefficient for a general slat type screen resulted from this part of the study.

The paper starts by describing the two selected numerical models. The study conducted to evaluate the damping screen loss coefficient is then introduced. This is followed by a description of the experimental program conducted on a number of TLDs. Results of the tests are used to assess the performance and range of applicability of the two numerical models with respect to the amplitude of applied excitation. Finally, the nonlinear model is used to study the influence of screen placement, number of screens inside the tank and the h/L value on the sloshing water response.

2. Analytical models of TLD equipped with damping screens

In the current study, both a linear model (Fediw et al., 1995) and a nonlinear model (Kaneko and Ishikawa, 1999) that simulate the sloshing fluid of a TLD equipped with damping screens are examined. For both models it is assumed that: the liquid is inviscid, irrotational and incompressible; the pressure is constant on the free surface; the quiescent water depth is constant; and the tank walls are rigid. Additionally, it is assumed that the water depth to tank length ratio, for a TLD equipped with damping screens, satisfies the shallow water wave theory limitation. Dean and Dalrymple (1984) suggest $h/L < 0.1$ but recognize that this limitation can be modified for particular applications. This will be verified by test results in this study.

2.1. Nonlinear model description

The nonlinear model of a TLD equipped with damping screens (Kaneko and Ishikawa, 1999) is briefly described below. Assuming the tank, shown in Fig. 1, is excited in a unidirectional motion, the nonlinear sloshing response can be expressed using shallow water theory as (Lepelletier and Raichlen, 1988)

$$\frac{\partial \eta}{\partial t} + \frac{\partial}{\partial x}[(h+\eta)u] = 0, \tag{1}$$

$$\frac{\partial u}{\partial t} + u\frac{\partial u}{\partial x} + g\frac{\partial \eta}{\partial x} - \frac{1}{3}(h+\eta)^2\frac{\partial^3 u}{\partial t \partial x^2} + \zeta_w u + \ddot{X} = 0, \tag{2}$$

where $\eta(x,t)$ is the free surface elevation, $u(x,t)$ is the horizontal velocity averaged through the fluid depth, L is the tank length, h is the still fluid depth, g is the gravitational acceleration, $\ddot{X}$ is the horizontal base acceleration, and ζ_w is the damping coefficient, proportional to the average velocity, introduced to account for the viscous dissipation (Miles, 1967).

The above continuity (1) and momentum (2) equations for nonlinear shallow water theory can be solved numerically, once the initial state of the fluid is prescribed, i.e., the values of u and h are given at time $t = 0$. A one-dimensional finite difference discretization scheme is applied for both u and η as shown in Fig. 2. The grid for u is staggered in a nonoverlapping fashion downstream to the η grid. The boundary conditions on the end walls of the tank are given as $u(-L/2,t) = u(L/2,t) = 0$. For a certain excitation amplitude, Eqs. (1) and (2) are integrated numerically using the Runge–Kutta–Fehlberg method after assigning the initial conditions for $\eta(x,0) = 0$ and $u(x,0) = 0$.

Using the method outlined by Kaneko and Ishikawa (1999) at locations where a damping screen is inserted (see Fig. 3), the velocity at a particular screen, U_{DSi}, can be expressed as

$$U_{DSi} = \frac{u_i + u_{i+1}}{2}. \tag{3}$$

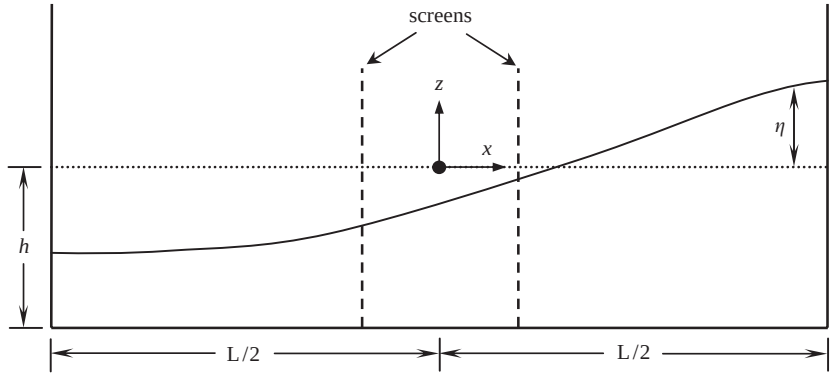

Fig. 1. Coordinate system for nonlinear shallow water model.

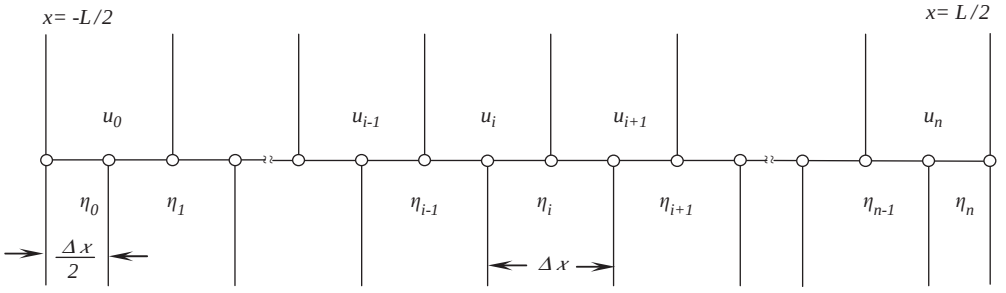

Fig. 2. Discretization of the tank length with respect to x.

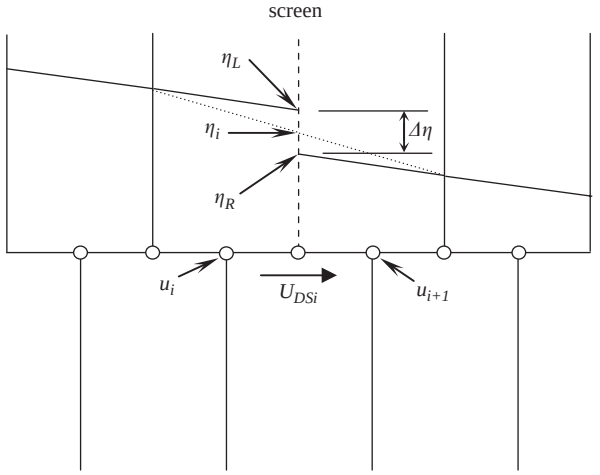

Fig. 3. Discretization and modelling of the screen.

The pressure drop, Δp, caused by the screen can be expressed as

$$\Delta p = C_l \frac{\rho U_{DSi}^2}{2}, \tag{4}$$

where C_l is defined as the pressure loss coefficient.

The relationship between the pressure loss coefficient and the free surface height difference across the screen is given by

$$|\eta_L - \eta_R| = \Delta\eta = C_l \frac{U_{DSi}^2}{2g}. \tag{5}$$

Upon integrating the discretized continuity and momentum equations with respect to time, the values of free surface on the left, η_L, and right, η_R, sides of the screen can be determined by

$$\eta_L = \eta_i + \text{sign}[U_{DSi}]\frac{\Delta\eta}{2}, \tag{6}$$

$$\eta_R = \eta_i - \text{sign}[U_{DSi}]\frac{\Delta\eta}{2}. \tag{7}$$

Subsequently, the velocity and the wave height can be determined with the influence of the damping screen taken into consideration.

2.2. Linear model description

The linear model developed by Fediw et al. (1995) for steady-state sinusoidal excitation is described below. It is assumed that u and η, the particle velocity and free surface elevation, and their derivatives are small quantities whose products and squares can be considered negligible in comparison with the linear terms. By applying these additional assumptions to the nonlinear shallow water equations, the well-known linear wave equation is obtained (Stoker, 1957), and is expressed here in terms of the particle displacement, e, as

$$\frac{\partial^2 e}{\partial x^2} - \frac{1}{gh}\frac{\partial^2 e}{\partial t^2} = 0. \tag{8}$$

From kinematics, the wave height, η, can be determined using the relation

$$\eta = -h\frac{\partial e}{\partial x}. \tag{9}$$

The tank is divided into a number of subtanks defined by the tank end walls and the screen locations, where N screens result in $N+1$ subtanks. For instance, a tank containing two screens ($N = 2$) would be divided into three subtanks

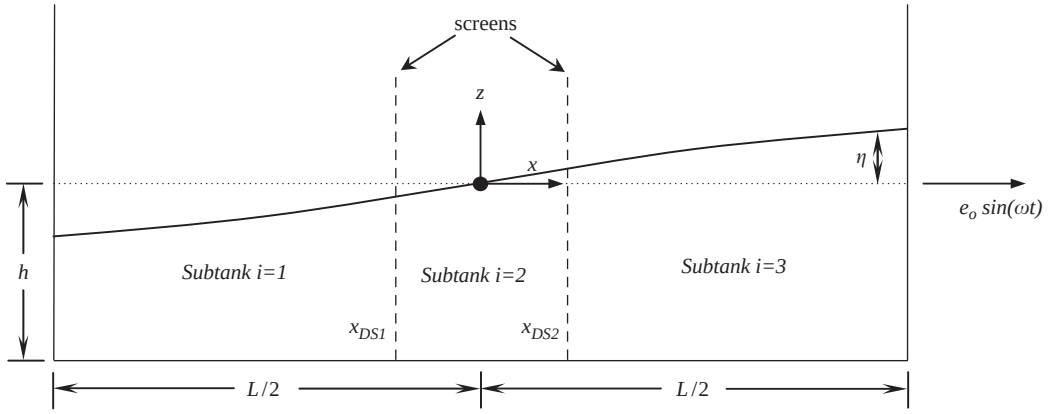

Fig. 4. Coordinate system and notation used for linear model.

($i = 3$) as shown in Fig. 4. In any subtank domain, the particle displacement, $e(x,t)$, satisfying Eq. (8) can be expressed as

$$e_i(x,t) = A_{4(i-1)+1}\cos\left(\frac{2\pi t}{T} - \frac{2\pi x}{\lambda}\right) - A_{4(i-1)+2}\cos\left(\frac{2\pi t}{T} + \frac{2\pi x}{\lambda}\right) + A_{4(i-1)+3}\sin\left(\frac{2\pi t}{T} - \frac{2\pi x}{\lambda}\right) + A_{4(i-1)+4}\sin\left(\frac{2\pi t}{T} + \frac{2\pi x}{\lambda}\right), \tag{10}$$

where λ is the wavelength and T is the period of excitation.

Regarding the boundary conditions, at the end walls the particle displacements are equal to the tank wall displacements. At each screen location, two boundary conditions are imposed. The first boundary condition states that at a certain screen location, x_{DSi}, the velocity into the screen is equal to the velocity out of the screen and is expressed as

$$\left(\frac{\partial e_i}{\partial t} = \frac{\partial e_{i+1}}{\partial t}\right)\Bigg|_{x=x_{DS_i}}. \tag{11}$$

The second boundary condition states that the head loss relationship across the screen is given by

$$\eta_{i+1} - \eta_i = C_u T\left(\frac{\partial e_{i+1}}{\partial t} - u_T\right)\Bigg|_{x=x_{DS_i}}, \tag{12}$$

where u_T is the tank velocity and C_u is defined as an equivalent linearized velocity loss coefficient and is given by

$$C_u = \frac{8}{3\pi}\frac{C_l}{2gT}\left|\left(\frac{\partial e_{i+1}}{\partial t} - u_T\right)\right|_{x=x_{DS_i}}. \tag{13}$$

A system of simultaneous equations results by applying the boundary conditions to each subtank domain. For the case of two screens, there are six boundary conditions (one for each end wall and two for each screen). Applying the above boundary conditions and equating coefficients results in 12 equations. The solution to the set of equations is obtained by employing an iterative method. An initial velocity loss coefficient is determined from an assumed velocity. At each screen location, the particle velocity is subsequently calculated using this assumed coefficient, and an updated velocity loss coefficient is calculated. The initially assumed velocity loss coefficient and the updated velocity loss coefficient are then compared. If the values are found to differ, the calculated velocity coefficient is updated and the iterative process is repeated until the velocity coefficient value converges to a unique solution.

3. Loss coefficient for slat type screens in oscillating flow

A pressure loss coefficient, C_l, for the slat screen utilized in this study is required for both the models described above. For steady flow (non-oscillating), Baines and Peterson (1951) suggest using the following equation

to estimate C_l:

$$C_l = \left(\frac{1}{C_c(1-S)} - 1\right)^2. \tag{14}$$

In the above equation, S is the solidity ratio of the screen that can be calculated as

$$S = \frac{A_s}{A_T}, \tag{15}$$

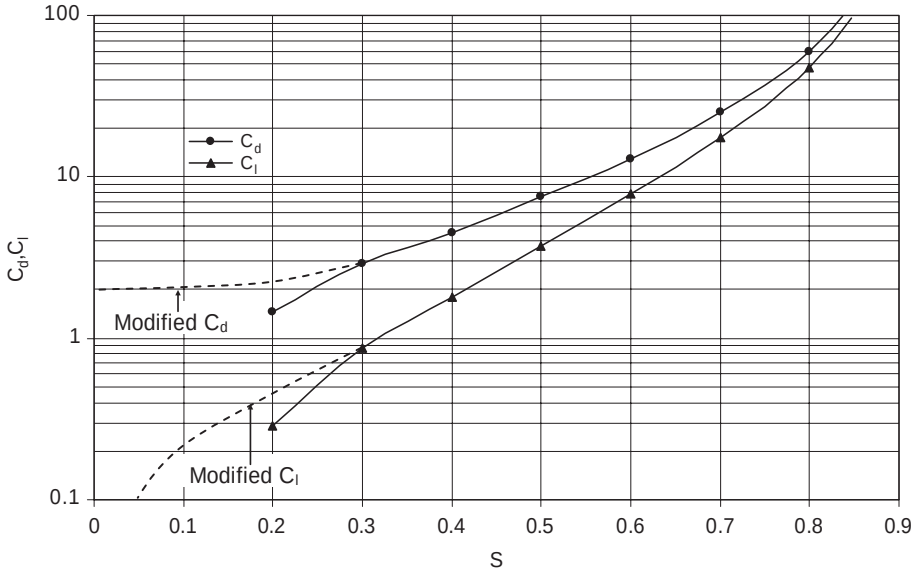

Fig. 5. Drag coefficient values for slat screens.

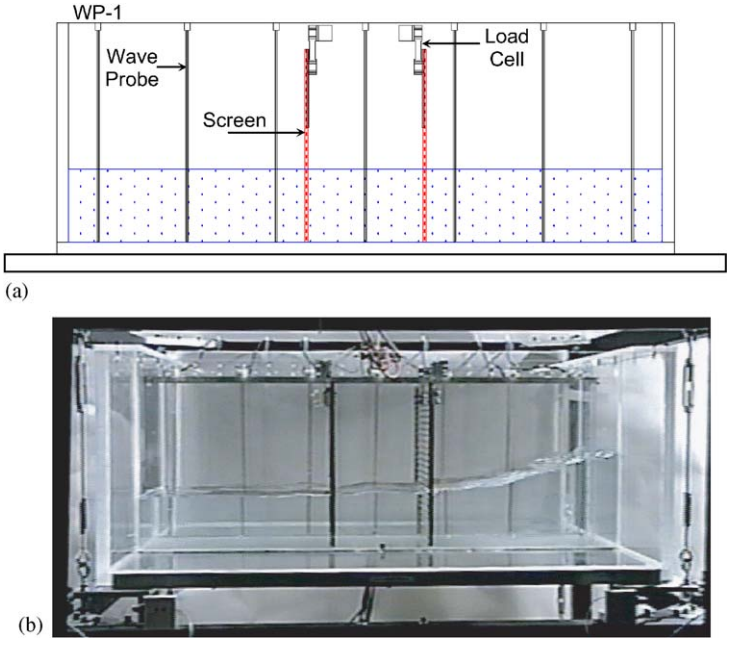

Fig. 6. (a) Schematic of experimental set-up and (b) photo ($A/L = 0.016$) of experimental test.

Table 1
Tuned liquid damper tank dimensions

Tank	L (mm)	b (mm)	h (mm)	(h/L)	f_w (Hz)
T1	966	360	119	0.123	0.545
T2	966	797	59.5	0.062	0.393
T3	797	966	160	0.200	0.740

where A_S is the solid portion of the screen submerged in water, A_T is the gross area of the screen submerged in water, and C_c is the contraction coefficient. The value of C_c for a thin plate orifice was measured experimentally by Weisbach (1855). An estimate of C_c can be made from the solidity ratio using the fitted equation

$$C_c = 0.405\mathrm{e}^{-\pi S} + 0.595. \tag{16}$$

The drag coefficient C_d is related to the loss coefficient C_l as follows:

$$C_d = \frac{C_l}{S}. \tag{17}$$

For a particular screen consisting of a number of thin plate slats and having a solidity ratio, S, Eqs. (14) and (17) can be used to estimate the coefficients C_l and C_d for that screen. A plot of C_l and C_d as functions of solidity is shown in Fig. 5. It should be noted that for solidity ratio values less than 0.3, the modified curves shown in Fig. 5 should be used (Baines and Peterson, 1951). Values of $C_d = 5.11$ and $C_l = 2.16$ are calculated for the screens used in this study.

3.1. Experimental evaluation of drag coefficient C_d

An experimental program is conducted in this part of the study to assess the applicability of the theoretically determined loss coefficient to the case of oscillating fluid motion experienced by a TLD during dynamic excitation. The experimental results are also used to check if the values of C_l are independent of the level of excitation as suggested by Eq. (14). The excitation amplitudes applied in this experimental study cover the practical range of serviceability accelerations for buildings subjected to wind loads as outlined by Isyumov (1994) and larger excitation amplitudes more representative of earthquake motion (Reed et al., 1998).

A tank is mounted to a shake table and subjected to a horizontal sinusoidal excitation in order to determine the drag coefficient, C_d, of the attached slat screens. The dimensions of the tank, denoted as $T1$, are presented in Table 1 where L is the tank length, b is the tank width, and h is the water depth. Two slat screens are attached to the tank at a distance $\pm 0.1L$ from the tank centre-line. Each screen has a solidity ratio $S = 0.42$. Based on linear wave theory, the natural frequency of the fundamental sloshing mode of the contained water is estimated to be 0.545 Hz. The forces on the screen are measured using load cells as shown in the experimental set-up in Figs. 6(a) and (b). The free surface elevation is recorded using seven wave probes providing a description of the free surface along the length of the tank. In addition, the table displacement is recorded using a laser displacement transducer. The TLD is excited sinusoidally at various excitation amplitudes near the estimated natural sloshing frequency.

The following procedure is used to estimate the value of C_d corresponding to a particular excitation amplitude and frequency near resonance.

1. The time history variation of the free surface measured by the seven wave probes are used to represent the free surface profile as a Fourier series at any instant in time (as shown in Fig. 7), i.e.,

$$\eta(x,t) = \sum_{n=0}^{6} \eta_n(t)\cos\left(\frac{n\pi x}{L}\right), \tag{18}$$

where

$$\eta_n(t) = \eta_n \cos(n\omega t) \tag{19}$$

and ω is the excitation frequency near resonance. Only the fundamental response component is retained, i.e., $n = 1$, for estimating the velocity at the screens. Therefore, η will be taken as η_1 and ω as the fundamental sloshing response in the following derivation.

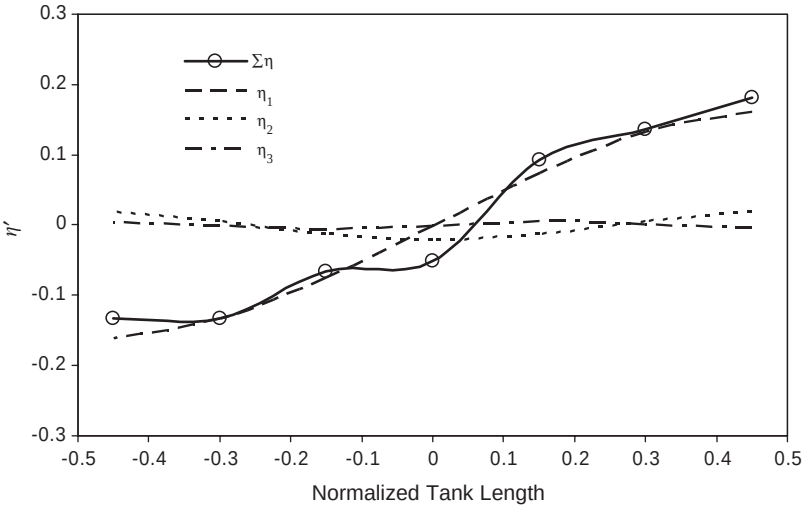

Fig. 7. Fourier series decomposition of the free surface profile.

2. The horizontal component of the water particle velocity, $u(x,z,t)$, for a standing wave can be obtained from the free surface amplitude as follows (Dean and Dalrymple, 1984):

$$u(x,z,t) = \eta\omega \frac{\cosh\left[\frac{\pi(z+h)}{L}\right]}{\sinh\left(\frac{\pi h}{L}\right)} \cos\left(\frac{\pi x}{L}\right) \cos(\omega t). \tag{20}$$

3. The above expression is integrated through the depth of the fluid, z, to obtain the average velocity $u(x,t)$

$$u(x,t) = \frac{\eta\omega L}{\pi h} \cos\left(\frac{\pi x}{L}\right) \cos(\omega t). \tag{21}$$

4. The coordinate ($x = x_{DS}$) at which the screen is located is substituted into Eq. (21) to obtain the average horizontal particle velocity amplitude, U_m, at that location.

As the screens are located in oscillating flow, the resulting motion of the water particles changes signs with each half-cycle of oscillation. According to Keulegan and Carpenter (1958), the drag coefficient of a plate can be obtained from the following relationship:

$$C_d = -\frac{3}{4} \int_0^{2\pi} \frac{F(\theta)\cos(\theta)}{\rho_w U_m^2 D} \, \mathrm{d}\theta, \tag{22}$$

where

$$\theta = \frac{2\pi t}{T}. \tag{23}$$

$F(\theta)$ is the periodic force measured by the load cells, T is the excitation period, ρ_w is the density of water, D is the slat width and U_m is the amplitude of the velocity at the screen location evaluated using Eq. (21).

The above procedure has been repeated over a range of A/L values varying from 0.0026 to 0.0414. The loss coefficients are found to be correlated with the period parameter often referred to as the Keulegan–Carpenter number (KC) defined as

$$KC = \frac{U_m T}{D}. \tag{24}$$

The KC provides a ratio between the amplitude of the particle motion to the size of the submerged body. As the value of KC increases, the case of steady flow is approached. Fig. 8 shows the values of C_d obtained from the experiments plotted as a function of KC. In addition, the drag coefficients obtained from two previous studies (Fediw, 1992;

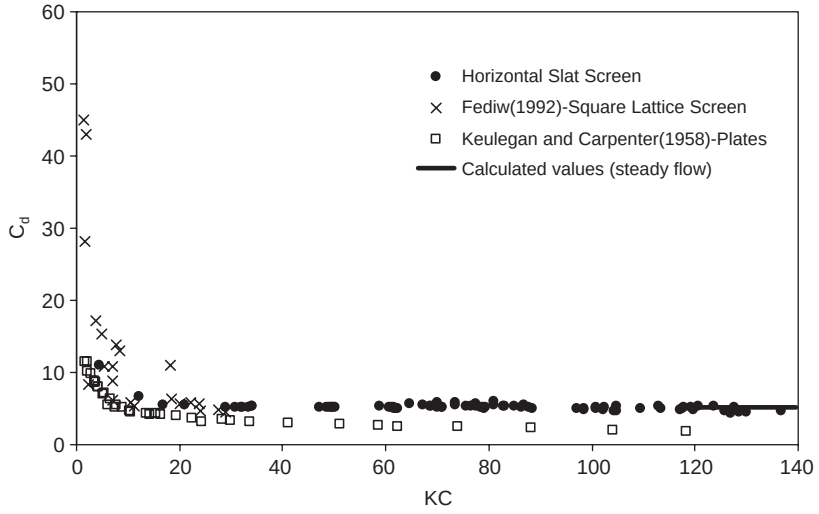

Fig. 8. Variation of drag coefficient with KC number.

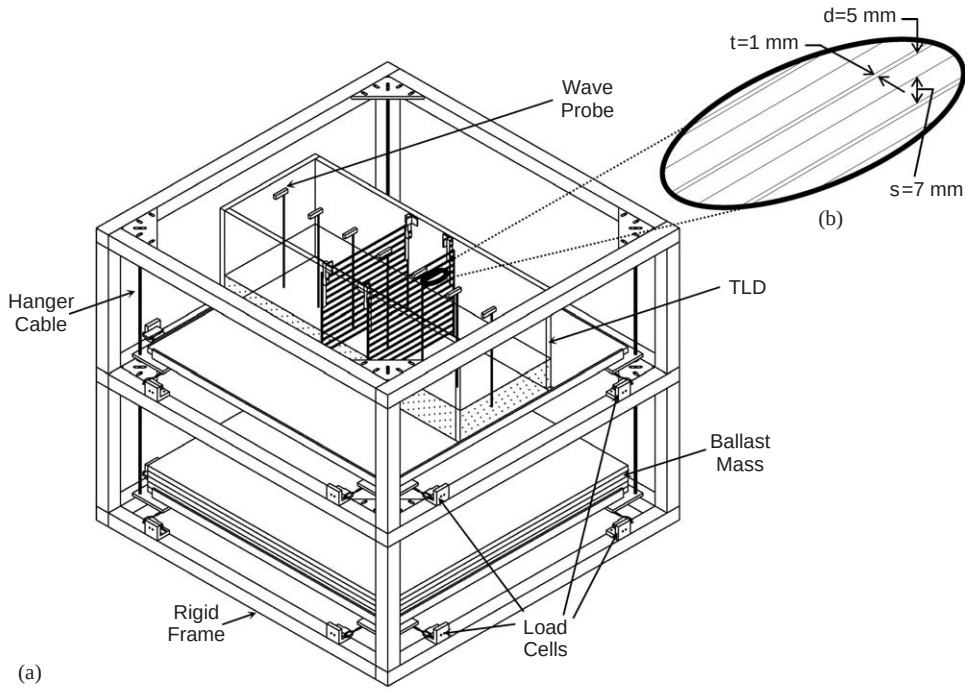

Fig. 9. Experimental set-up showing (a) TLD rigid test frame and load cells and (b) TLD damping screens.

Keulegan and Carpenter, 1958) have been plotted as an indicator of expected trends. Results show that the drag coefficient increases for small KC values, matching the trend found by previous studies. For KC values greater than approximately 15, the drag coefficient is found to maintain a near-constant value of approximately 5.1. Also shown in this figure is the calculated value of C_d obtained from Eqs. (14)–(17) for the slat screen in steady flow, which is found to be in excellent agreement with experimental values for KC larger than 15. It can be concluded from the experimental results that the drag coefficient obtained from steady flow using the procedure described above can be used for the slat screens for both small and large excitation amplitudes.

Table 2
Experimental test description

Test series number	Test case	Tanks tested	Number of screens	Screen location (% L)	Normalized excitation amplitudes (A/L)	Purpose
1	A	T1	2	± 10	0.003–0.041	Assess the effect of excitation amplitude
2	A	T1	2	± 10	0.003–0.041	Assess the effect of screen location and number of screens
	B		2	± 20	0.005–0.021	
	C		2	± 25	0.010–0.021	
	D		3	± 25 and 0	0.01	
3	A	T1	2	± 10	0.005–0.031	Assess the effect of h/L
	B	T2	2	± 10	0.016	
	C	T3	2	± 10	0.019	

4. Experimental study to assess the numerical models

A series of experimental tests are carried out in order to investigate three parameters, namely the effect of: (1) excitation amplitude, (2) number of screens/screen location, and (3) h/L ratio. The details of the test program are provided in Table 2. The experimental set-up used for this investigation is shown in Figs. 9(a) and (b). The data measured include the shake table displacement using a laser transducer, the sloshing base shear forces in the direction of excitation using load cells, and the temporal water surface variations at seven locations using wave probes. In presenting the results, the following parameters are used:

excitation frequency ratio, β_w,

$$\beta_w = \frac{f}{f_w}, \tag{25}$$

where f_w is the fundamental natural frequency of the water sloshing motion predicted by the linear wave theory and given as

$$f_w = \frac{1}{2\pi}\sqrt{\frac{\pi g}{L}\tanh\left(\frac{\pi h}{L}\right)} \tag{26}$$

and f is the excitation frequency;

nondimesional free surface response elevation, η',

$$\eta' = \frac{\eta}{h}; \tag{27}$$

nondimensional base shear forces, F'_w,

$$F'_w = \frac{F_w}{m_w A\omega^2}, \tag{28}$$

where F_w is the reaction force that develops from the sloshing fluid motion and the denominator represents the maximum inertial force of the water mass treated as a solid mass;

nondimensional energy dissipation per cycle, E'_w,

$$E'_w = \frac{E_w}{\frac{1}{2}m_w(A\omega)^2}, \tag{29}$$

where the denominator is the maximum kinetic energy of the water mass treated as a solid mass and the numerator is the energy dissipated per cycle defined as

$$E_w = \int_t^{t+T} F_w \,\mathrm{d}x(t). \tag{30}$$

4.1. Effect of excitation amplitude

Both time history analysis and frequency analysis are performed to examine the performance of both models. Results from test series (1) are used to assess the ability of the analytical models to simulate the free surface profile, the resulting base shear force, and the energy dissipated by the TLD.

4.2. Time history response comparisons

The response wave forms for the free surface motion and the base shear forces, calculated from the analytical models, are compared with experimental results from test series (1) over a range of excitation amplitudes and excitation frequencies. The free surface variation near the end wall, measured using probe WP-1 is plotted in Fig. 10 for A/L values of 0.005, 0.016, and 0.031 at an excitation frequency ratio of $\beta_w = 1.01$. Also shown is the predicted free surface time histories generated by the linear and nonlinear analytical models. Good agreement for the maximum free surface amplitude (wave crest) is found to occur between the nonlinear model and the experimental data for all excitation amplitudes. Some discrepancy is found to occur as the free surface approaches its minimum value (wave trough), where high-frequency trailing waves occur as observed in experiments conducted here and by others (Reed et al., 1998). Since the linear model is not capable of simulating the nonlinear free surface response, significant discrepancies are expected to be found between the experimental results and the linear simulations. As a result, the linear model underestimates the maximum free surface response and overestimates the minimum free surface response. The linear model underestimates the maximum wave height by a factor of approximately 1.4 and 2.4 for the 0.005 and 0.031 amplitude cases, respectively.

Fig. 11 shows the resultant normalized base shear force that develops from the sloshing water motion. Good agreement is found between the nonlinear model and the experimental data for all three excitation amplitudes. The linear model is in good agreement with the experimental results at the 0.005 excitation amplitude ratio. Greater discrepancy is found to occur between the linear model and the experimental results at 0.016 excitation amplitude ratio. For $A/L = 0.031$, the linear model underestimates the shear force by approximately 15%. By comparing Figs. 10 and 11, it is evident that the base shear forces do not display the same degree of nonlinearity as the free surface motions. This allows the resultant base shear forces to be accurately modelled by a linear model at lower excitation amplitudes.

4.3. Frequency response comparisons

Fig. 12 shows both the experimentally and numerically simulated nondimensional energy dissipation frequency response curves for three excitation amplitude ratios which are obtained at each excitation frequency using Eqs. (29) and (30). It is evident from the multi-peaked frequency response curves shown in the figure that the nonlinear flow model is able to simulate the nonlinear response of the TLD. The dissipated energy as predicted by the nonlinear model is in good agreement with the data obtained experimentally, although a small frequency shift is observed. The nonlinear model overpredicts the energy dissipated for the 0.031 amplitude ratio case for certain excitation frequencies. The linear flow model is unable to capture the influence of the nonlinearities on the fundamental sloshing response. The linear model overpredicts the energy dissipated by the TLD near resonance for all three excitation amplitudes investigated. Although the linear model results show greater deviation from the experimental values compared to the nonlinear model, it does allow an initial estimate of the energy dissipated by the TLD with screens to be made. An estimate of ζ_{TLD} can be made from the nondimensional energy dissipation plots shown in Fig. 12 (Tait et al., 2004a). Generally, as the energy dissipation curve increases in height and decreases in width the value of ζ_{TLD} decreases. The estimated ζ_{TLD} values for the 0.016 amplitude ratio are 11.8%, 11.7%, and 11.0% for the experimentally measured, nonlinear model, and linear model, respectively. From these results it can be concluded that the linear model can be used to initially size and place the damping screens inside the tank and estimate ζ_{TLD}. After a screen arrangement has been decided upon, including the solidity ratio and screen locations, the nonlinear model can be used to validate the design and provide a more accurate estimate of the TLD response. Additionally, the nonlinear model is validated for use in both wind loading applications where the excitation amplitudes are small and large excitation amplitudes that are more representative of earthquake loading.

4.4. Effect of screen placement

The effect of screen placement and the number of screens inside the tank on the performance of a TLD are investigated and reported in this section. Experimental results from test series (2) are used to validate the nonlinear

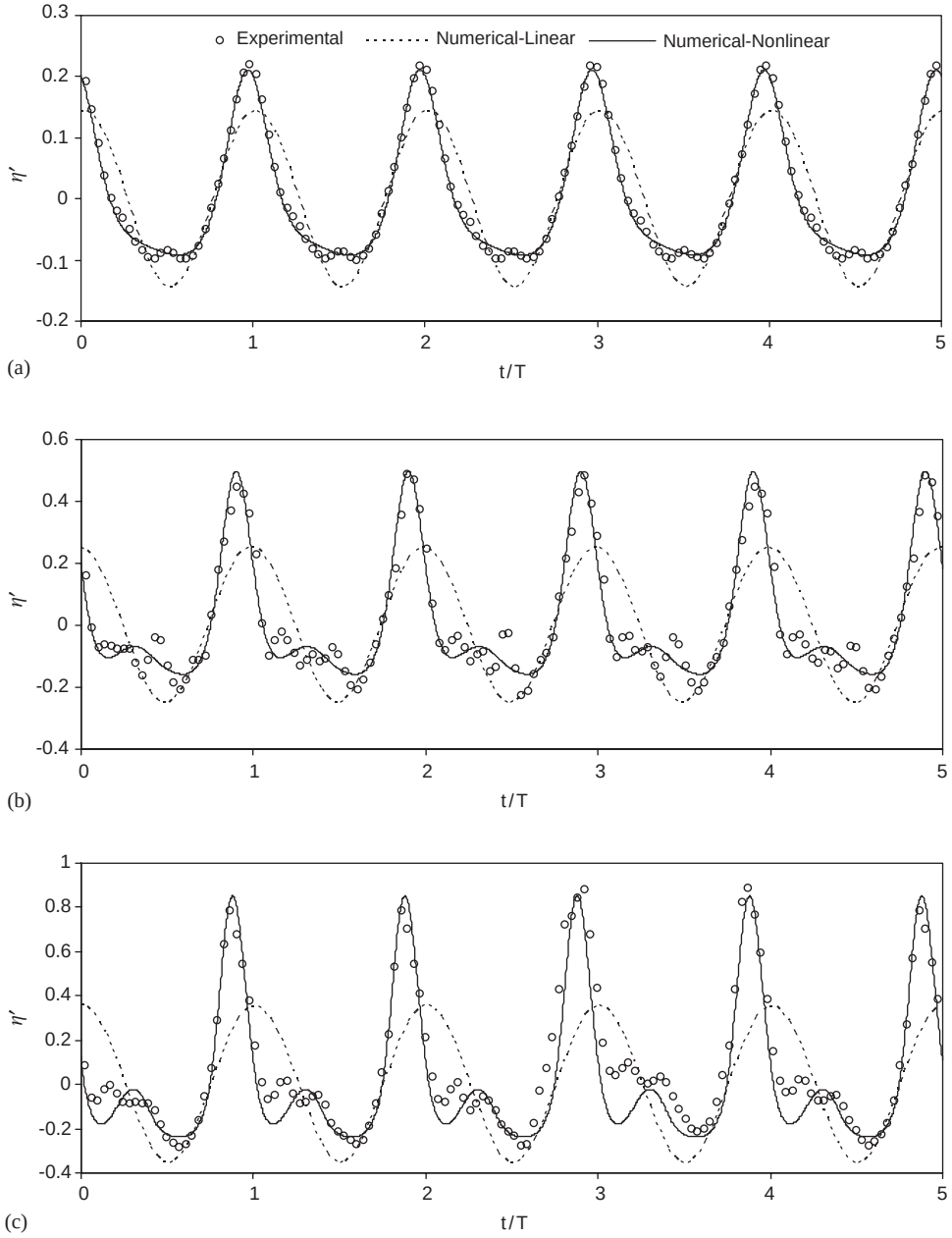

Fig. 10. Comparison of experimental to calculated normalized free surface at end wall for A/L values of (a) 0.005, (b) 0.016, (c) 0.031.

model's ability to simulate the sloshing response of a TLD having different screen arrangements. Fig. 13 shows the normalized velocity amplitude, Γ, along the tank length for first three linear sloshing modes calculated using linear wave theory. Placing a screen at the centre, where maximum velocity occurs for the first sloshing mode, would result in the highest losses across the screen for this particular sloshing mode as the pressure loss across the screen is proportional to the square of the velocity. However, negligible losses occur in the second mode for this same screen location as the velocity is zero at the centre of the tank for the second sloshing mode. Four screen arrangements, detailed in Table 2, are configured to study the influence of screen location on the sloshing response. Test case 2A corresponds to locations where the normalized velocity amplitude is large for the first mode and has equal values for the second and third modes. Test case 2B corresponds to locations where the velocity is significant for both the first and the second sloshing modes.

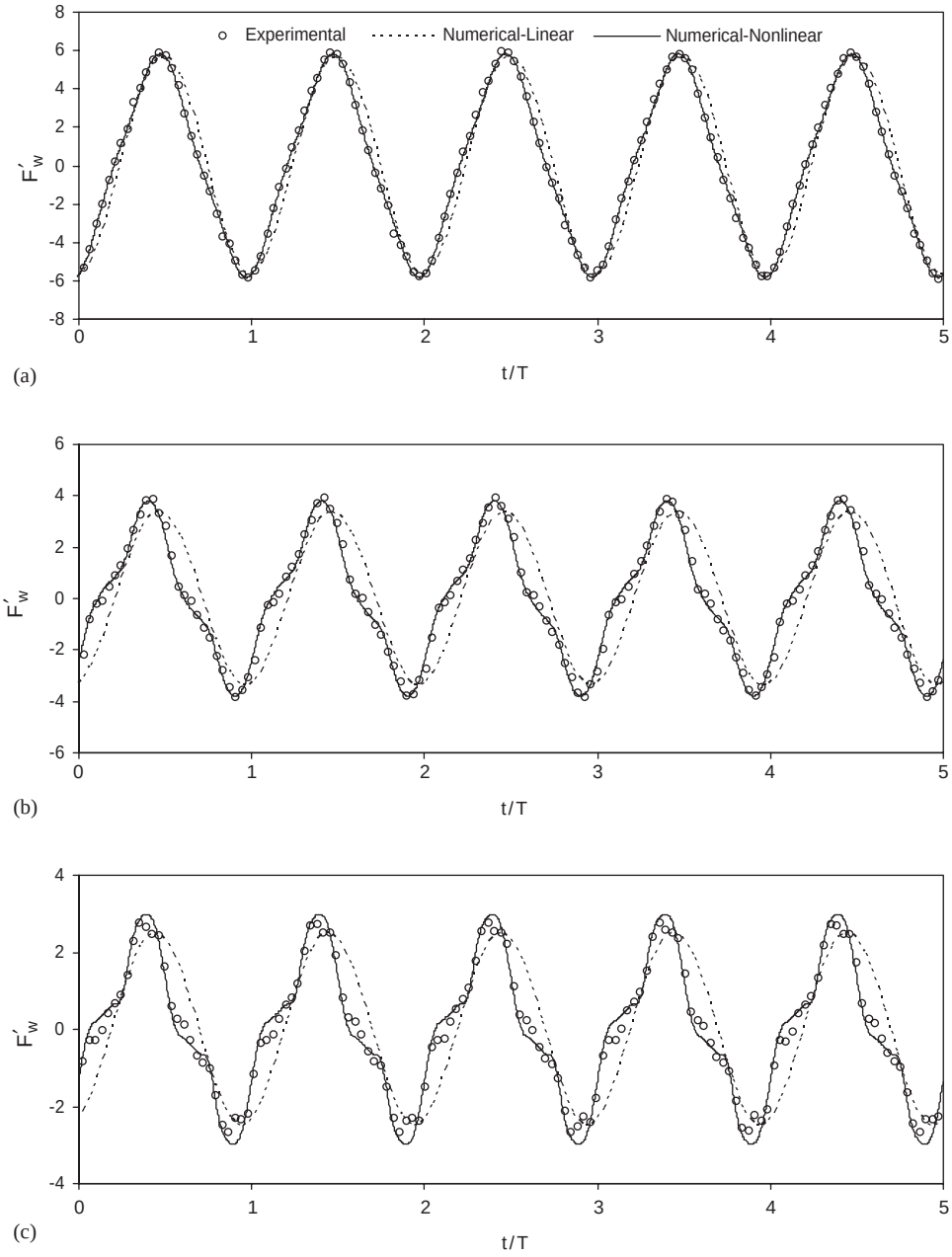

Fig. 11. Comparison of experimental and calculated normalized base shear forces for A/L values of (a) 0.005, (b) 0.016, (c) 0.031.

Test case 2C corresponds to the location where the second mode has the largest velocity value and the first and third normalized velocity amplitudes are equal. The fourth configuration, test case 2D consisting of three screens, is studied to examine the influence of adding an additional screen at the centre of the tank to case 2C.

The energy dissipation frequency response curves for the four configurations are presented in Fig. 14. Comparing the three two-screen test cases, the maximum value of E'_w is found to increase as the two screens are moved further away from the centre of the tank. An increase in the height and decrease in width of the E'_w response curve indicates a decrease in ζ_{TLD}. This result is expected as the sloshing response is dominated by fundamental sloshing mode, which results in the greatest fluid velocity occurring at the centre of the tank. Both the peak value of the dissipation curves and

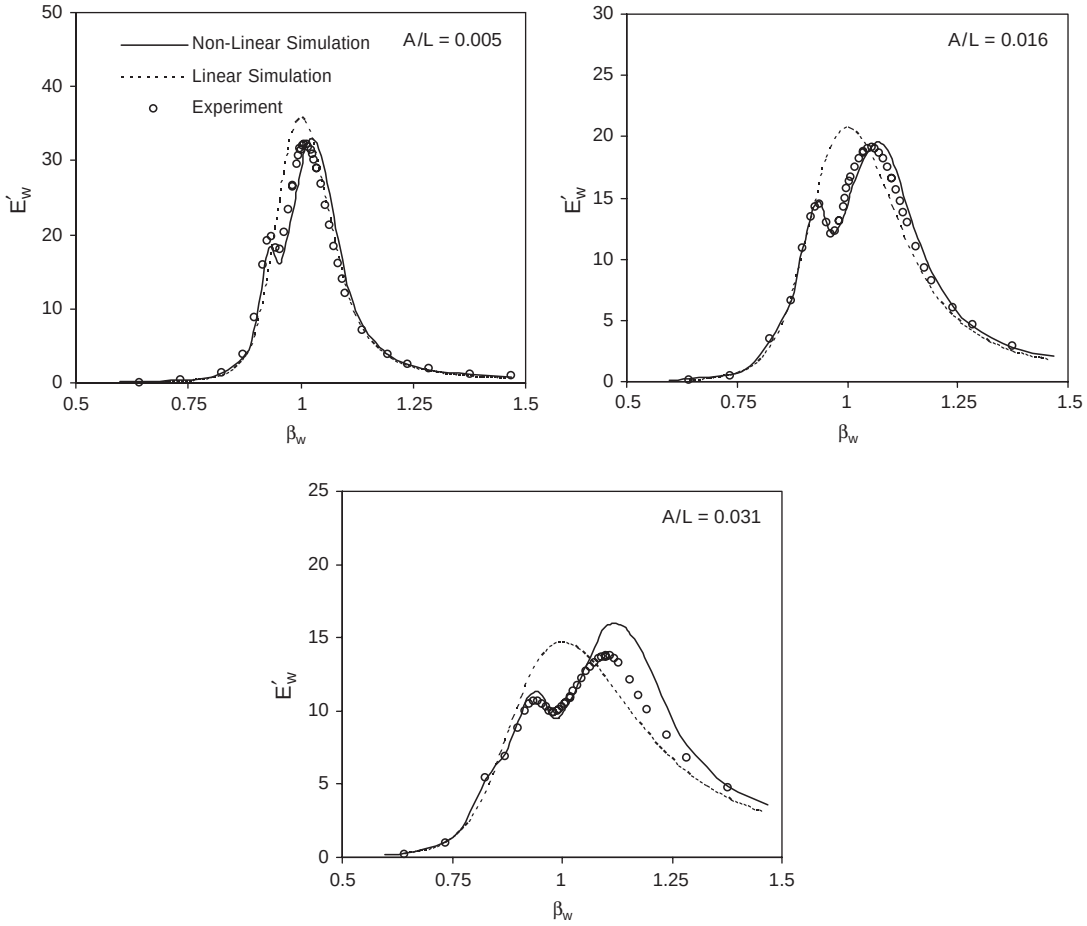

Fig. 12. Experimental and numerical results for TLD energy dissipation.

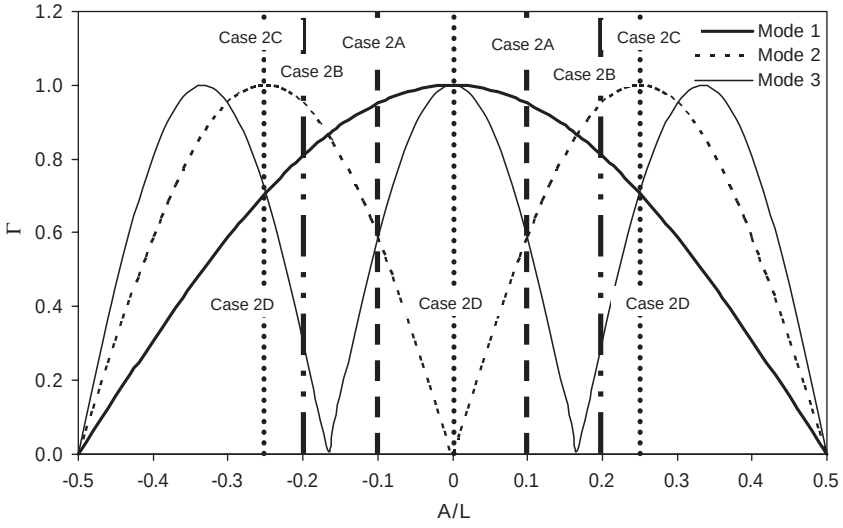

Fig. 13. Estimated normalized fluid velocity for the first three sloshing modes and screen locations inside the tank.

the shape of the response curve are found to change with screen placement. The reduction of the secondary peak in frequency response curves indicates that placing screens in locations where the velocity is greatest for higher sloshing modes aids in suppressing the nonlinear response. The greatest reduction in the E'_w response curve is found for the three-screen case (test case 2D). This response curve also displays the least amount of distortion from the influence of the nonlinearities.

For all four test cases, the nonlinear model is able to simulate the experimental results. Therefore, the nonlinear model is capable of modelling multiple screens at multiple locations. It can be concluded from the results that the screen location and number of screens can be selected to increase damping and additionally suppress the presence of higher sloshing response harmonics due to nonlinearities. In the case where the required amount of inherent damping of the TLD requires a screen having a solidity ratio that impedes the fluid motion too significantly, a multiple screen configuration may be implemented.

4.5. Influence of tank length to fluid depth (h/L) ratio

Tests were conducted on three different tanks having different h/L values as indicated for test series (3) shown in Table 2. This experimental investigation was conducted to validate the nonlinear model using multiple screens over a

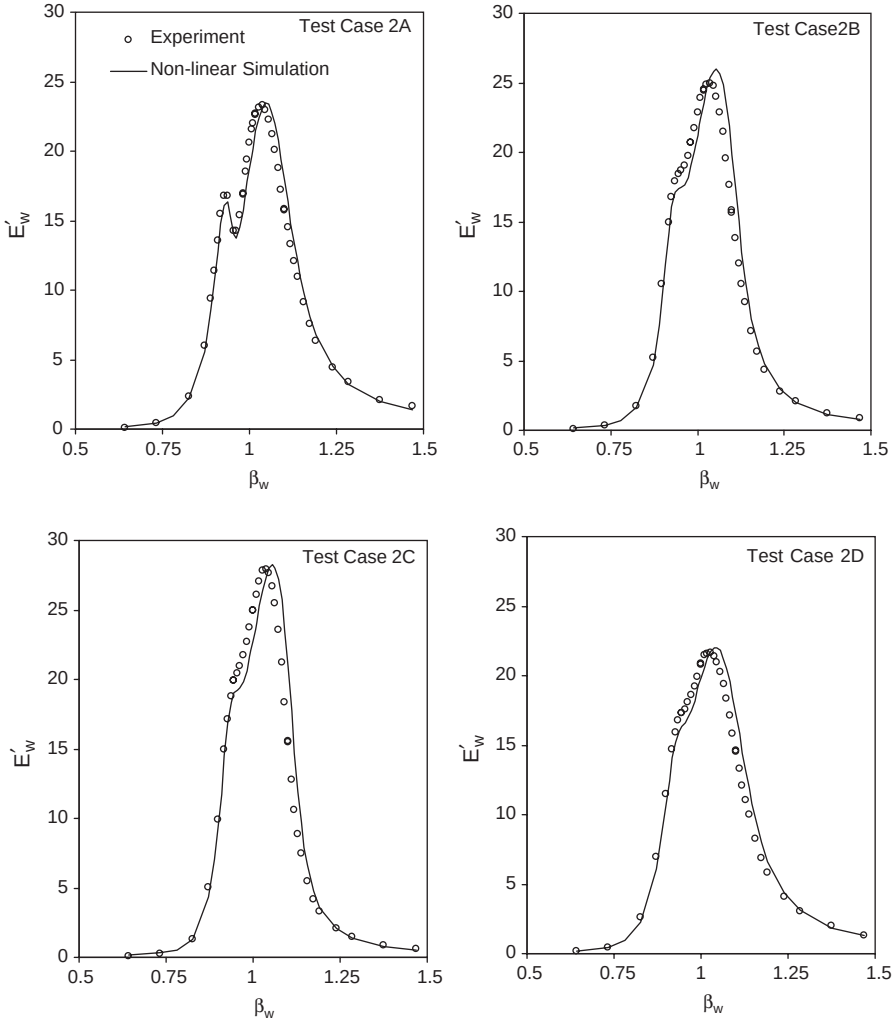

Fig. 14. Influence of screen placement on TLD energy dissipation and numerical model comparison.

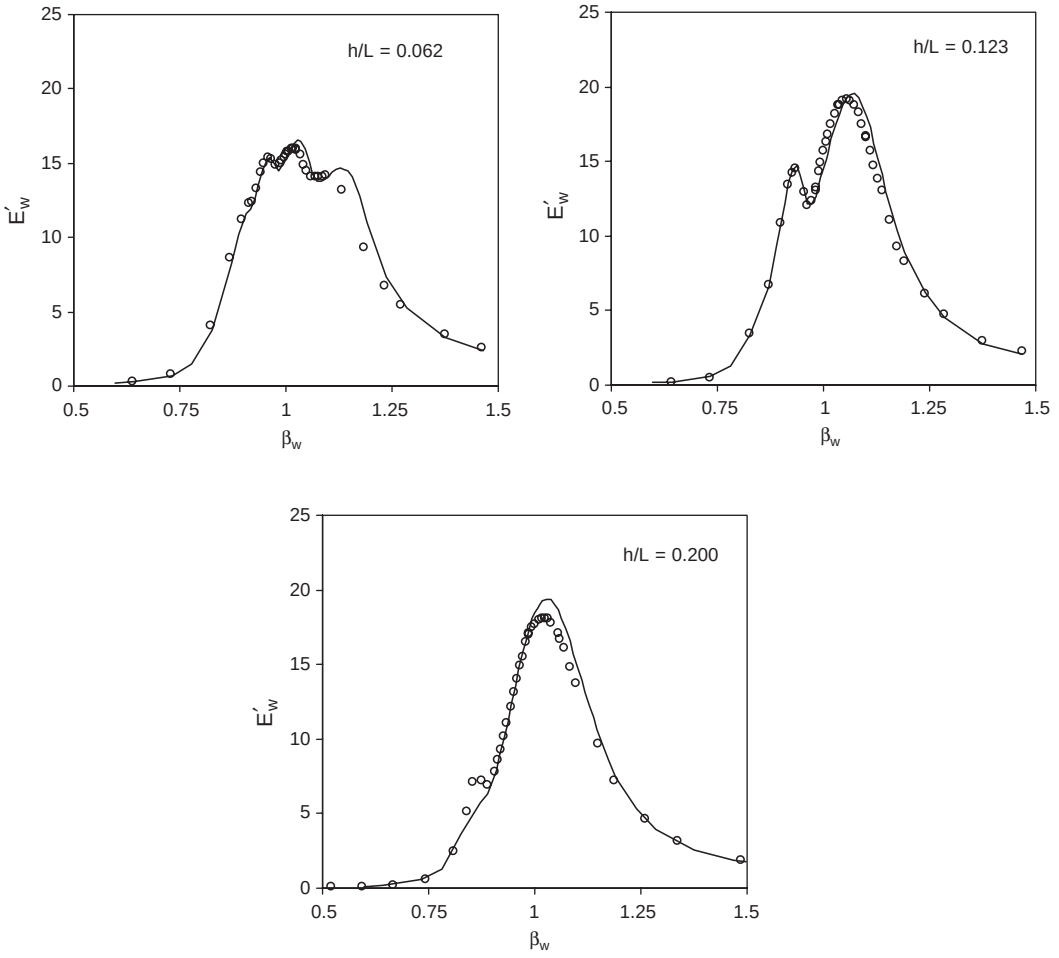

Fig. 15. Influence of h/L on TLD energy dissipation and model predictions.

range of h/L values at excitation amplitudes not investigated previously. The experimental results are plotted in Fig. 15 along with the numerical simulations from the nonlinear model. The influence of the nonlinearities on the fundamental sloshing mode, resulting in a multi-peaked frequency response curve decreases as h/L is increased, as seen in Fig. 15. However, with greater fluid depth, less water participates in sloshing, reducing the performance of the TLD. The nonlinear numerical model is found to provide satisfactory results for all three h/L values. Some deviation between the experimental and numerical simulations is found to occur for $h/L = 0.200$. It is expected that as h/L increases, the model's performance will decrease as the model is based on shallow water wave theory. From these results it can be concluded that the numerical model can be used in designing TLD devices over a significant range of h/L values up to $h/L = 0.200$ with multiple screens placed inside the tank.

5. Conclusions

In this paper both linear and nonlinear numerical modelling of a TLD with slat screens have been conducted and verified by a comprehensive experimental study. A procedure to calculate the theoretical value of the force coefficient of a slat-type screen is presented and verified from experimental results. Findings indicate that the loss coefficient of slat screens in oscillating flow can be estimated from screen loss values obtained in steady flow for KC larger than

approximately 15. The suggested method for determining the slat screen loss coefficients is applicable for both wind (small excitation) and earthquake (large excitation) loading.

Both the linear and nonlinear analytical models for TLDs are examined and compared with experimental data. Findings indicate that the linear model is capable of providing a first estimate of the energy dissipating characteristics of a TLD. However, the linear model does not provide realistic estimates of the free surface response for amplitudes experimentally investigated. The nonlinear model can accurately describe the free surface motion, the resulting base shear forces and the energy dissipated over a range of excitation amplitudes. The nonlinear model is capable of modelling a TLD equipped with multiple screens at various screen locations inside the tank. The nonlinear model is also verified over a range of practical fluid depth to tank length ratio values. Using the procedure outlined in this paper, slat screens can be sized and positioned according to the linear model results. Once the target energy dissipation frequency response curve and consequently the required value of ζ_{TLD} have been estimated from the linear model, a more detailed study of the TLD response characteristics can be made using the nonlinear model.

Acknowledgements

The authors would like to thank Dr J.D. Kim for many valuable discussions regarding the numerical modelling and the technical staff at the Boundary Layer Wind Tunnel Laboratory at the University of Western Ontario for their assistance during experiments. This study was partially supported by the Natural Sciences and Engineering Council of Canada (NSERC).

References

Baines, W.D., Peterson, E.G., 1951. An investigation of flow through screens. ASME Transactions 73, 467–479.

Dean, R.G., Dalrymple, A.D., 1984. Water Wave Mechanics for Engineers and Scientists, first ed. Prentice-Hall Inc., Englewood Cliffs, NJ.

Fediw, A.A., 1992. Performance of a one dimensional tuned sloshing water damper. M.E.Sc. Thesis, University of Western Ontario, London, Canada.

Fediw, A.A., Isyumov, N., Vickery, B.J., 1995. Performance of a tuned sloshing water damper. Journal of Wind Engineering and Industrial Aerodynamics 57, 237–247.

Fujino, Y., Pacheco, B.M., Chaiseri, P., Sun, L.M., 1988. Parametric studies on tuned liquid damper (TLD) using circular containers by free-oscillation experiments. Structural Engineering/Earthquake Engineering, JSCE 5, 381s–391s.

Isyumov, N., 1994. Criteria for acceptable wind induced motions. In: Proceedings of the 12th Structures Congress, Georgia.

Kaneko, S., Ishikawa, M., 1999. Modeling of tuned liquid damper with submerged nets. ASME Journal of Pressure Vessel Technology 121, 334–343.

Keulegan, G.H., Carpenter, L.H., 1958. Forces on cylinders and plates in an oscillating fluid. Journal of Research of the National Bureau of Standards 60, 423–440.

Lepelletier, T.G., Raichlen, F., 1988. Nonlinear oscillations in rectangular tanks. ASCE Journal of Engineering Mechanics 114, 1–23.

Miles, J.W., 1967. Surface wave damping in closed basins. In: Proceedings of the Royal Society of London, vol. 297, pp. 459–475.

Noji, T., Yoshida, H., Tatsumi, E., Kosaka, H., Hagiuda, H., 1988. Study on vibration control damper utilizing sloshing of water. Journal of Wind Engineering, Japan Association for Wind Engineering 37, 557–566.

Reed, D., Yu, J., Yeh, H., Gardarsson, S., 1998. Investigation of tuned liquid dampers under large amplitude excitation. ASCE Journal of Engineering Mechanics 124, 405–413.

Stoker, J.J., 1957. Water Waves: The Mathematical Theory with Applications. Interscience Publishers Inc., New York, NY.

Sun, L.M., Fujino, Y., Pacheco, B.M., Chaiseri, P., 1992. Modelling of tuned liquid damper (TLD). Journal of Wind Engineering and Industrial Aerodynamics 41-44, 1883–1894.

Tait, M.J., El Damatty, A.A., Isyumov, N., 2004. Testing of tuned liquid damper with screens and development of equivalent TMD model. Wind and Structures, An International Journal 7, 215–234.

Tamura, Y., Fujii, K., Ohtsuki, T., Wakahara, T., Kohsaka, R., 1995. Effectiveness of tuned liquid dampers under wind excitation. Engineering Structures 17, 609–621.

Warburton, G.B., 1982. Optimum absorber parameters for various combinations of response and excitation parameters. Earthquake Engineering and Structural Dynamics 10, 381–401.

Warnitchai, P., Pinkaew, T., 1998. Modelling of liquid sloshing in rectangular tanks with flow-dampening devices. Engineering Structures 20, 593–600.

Weisbach, J., 1855. Die Experimental-Hydraulik. Englehardt, Freiburg.

Welt, F., 1983. A Parametric Study of Nutation Dampers. M.A.Sc. Thesis, University of British Columbia, BC, Canada.